

Organic & Biomolecular Chemistry

Accepted Manuscript



This article can be cited before page numbers have been issued, to do this please use: A. Campisi, M. A. Chiacchio, L. Legnani, P. Bottino, G. Lanza, D. Iannazzo, L. Veltri, S. V. Giofrè and R. ROMEO, *Org. Biomol. Chem.*, 2019, DOI: 10.1039/C9OB00651F.



This is an Accepted Manuscript, which has been through the Royal Society of Chemistry peer review process and has been accepted for publication.

Accepted Manuscripts are published online shortly after acceptance, before technical editing, formatting and proof reading. Using this free service, authors can make their results available to the community, in citable form, before we publish the edited article. We will replace this Accepted Manuscript with the edited and formatted Advance Article as soon as it is available.

You can find more information about Accepted Manuscripts in the [author guidelines](#).

Please note that technical editing may introduce minor changes to the text and/or graphics, which may alter content. The journal's standard [Terms & Conditions](#) and the ethical guidelines, outlined in our [author and reviewer resource centre](#), still apply. In no event shall the Royal Society of Chemistry be held responsible for any errors or omissions in this Accepted Manuscript or any consequences arising from the use of any information it contains.

1,2,4-OXADIAZOLE-5-ONES AS ANALOGUES OF TAMOXIFEN: SYNTHESIS AND BIOLOGICAL EVALUATION

View Article Online
DOI: 10.1039/C9OB00651F

Maria A. Chiacchio,^a Laura Legnani,^a Agata Campisi,^{*a} Bottino Paola,^a Lanza Giuseppe,^a Daniela Iannazzo,^b Lucia Veltri,^c Salvatore Giofrè^d and Roberto Romeo^d

^a Dipartimento di Scienze del Farmaco, Università di Catania, Viale A. Doria 6, 95125 Catania, Italy.

^b Dipartimento di Ingegneria, Università di Messina, Contrada Di Dio, 98166 Messina, Italy.

^c Dipartimento di Chimica e tecnologie chimiche, Università della Calabria, Via P. Bucci 12/C, 87036 Arcavacata di Rende, Italy.

^d Dipartimento di Scienze chimiche, biologiche, farmaceutiche ed ambientali, Università di Messina, Via S.S. Annunziata, 98168 Messina, Italy.

Abstract. A series of 2,3,4-triaryl-substituted 1,2,4-oxadiazole-5-ones have been prepared as fixed-ring analogues of tamoxifen (TAM), a drug inhibitor of Estradiol Receptor (ER) used in breast cancer therapy, by an efficient synthetic protocol based on a 1,3-dipolar cycloaddition of nitrones to isocyanates. Some of new synthesized compounds (**14d-f**, **14h** and **14k**) show a significant cytotoxic effect in human breast cancer cell line (MCF-7) possessing IC₅₀ values between 15.63 and 31.82 μM. In addition, compounds **14d-f**, **14h** and **14k** are able to increase the p53 expression levels, activating also the apoptotic pathway. Molecular modeling studies of novel compounds performed on the crystal structure of ER, reveal the presence of strong hydrophobic interactions with the aromatic rings of the ligands similar to TAM. These data suggest that 1,2,4-oxadiazole-5-ones can be considered analogues of TAM, and that their anticancer activity might be partially due to ER inhibition.

1. Introduction

Breast cancer is the most commonly diagnosed disease among women worldwide with over 2 million of new cases in 2018.¹ Many experimental and clinical evidences point out that other than genetic factors, steroid hormones play an important role in the etiology of this disease.²

Estrogen mediates its effects by binding to its receptors, ER α and ER β , and support the development and growth of the breast tumor cells and show also profound and carefully regulated effects on other tissues, such as the endometrium, vagina, bone, liver and vessels of the cardiovascular system.³

ER, interacting with estrogen response elements (EREs) contained in the promoter region of specific genes, modulates gene expressions that results in their biological effects. Extracellular signals can also stimulate ER α -mediated transcription in the absence of estrogen.

In recent years, emerging evidence has revealed that a role for ER α is to affect gene expression in the absence of direct DNA binding. In addition, ER activity in breast cancer is associated with drug resistance, tumor growth, increased invasiveness, poor patient prognosis, and loss of p53 function.⁴ Tumor suppressor protein p53 plays a key role in regulation of several cellular processes, including apoptosis, DNA repair and angiogenesis; it is a direct transcriptional target of ER α and modulates DNA damage-induced growth in breast cancer cells.⁵

A great number of estrogens antagonists (antiestrogens) have been synthesized and tested with regard to their binding affinity to the ER, a ligand-activated transcription factor that act by binding to EREs.⁶ The assumption that the utilization of estrogen antagonists for the treatment of breast cancers is capable of avoiding the progress of the disease has attracted considerable interest:⁷ pharmacological inhibition of the tumor stimulatory effects of physiological estrogens by an antiestrogen therapy was reported since the 1940s.

Several findings demonstrated that synthetic efforts have led to the discovery and development of various potent synthetic antiestrogens, many of them characterized by a stilbene-like skeleton such as Tamoxifen (TAM).⁸

TAM **1**, a non-steroidal, triphenylethylene-based compound (Fig. 1), has a complex pharmacology consisting of both estrogenic and anti-estrogenic properties in several tissues.⁹ This drug has revolutionized the treatment of breast cancer and it is considered the antiestrogen of choice in the clinic to date. It inhibits proliferation and induces apoptosis in ER-positive breast cancer cell line MCF-7, by selective estrogen receptor (ER)-dependent modulation of gene expression.¹⁰ After oral administration, TAM is converted, by cytochrome P₄₅₀ metabolism, into 4-hydroxytamoxifen **2** and 4-hydroxy-*N*-desmethyltamoxifen **3** (Fig. 1), potent antagonists of ERs and inhibitors of estrogen-responsive gene transcription.¹¹

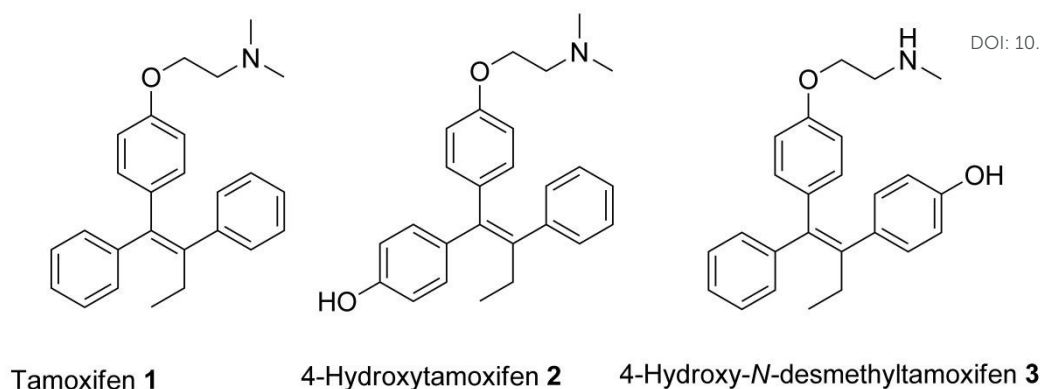


Fig. 1 Tamoxifen and its metabolites with anti-estrogenic activity.

Since TAM **1** and its metabolites **2** and **3** contain a double bond, formation of *E* and *Z* isomers can occur, with remarkably different binding affinities and effects at ER. For example, *Z*-TAM binds to ER with a 100-fold greater affinity than *E*-TAM: *Z*-TAM acts as an ER antagonist, while *E*-TAM acts as an ER agonist.¹² Similar differences in affinity and activity have also been observed with metabolites **2** and **3**:¹³ (*Z*)-4-hydroxytamoxifen exhibits an 8-fold higher binding affinity to the ER as compared to TAM, whereas the (*E*) isomer has only a 5% affinity to the ER.¹⁴ TAM also can induce side effects, such as the uterine endometrial cancer and the non-alcoholic fatty liver disease. These effects are a substantial concern for patients that have to continue TAM treatment for up to 10 years.¹⁵ Thus, after the approval of TAM for the treatment of breast cancer, considerable research efforts have been devoted towards the design and the discovery of novel TAM analogs with increased binding affinity for ER, able to combat the often reported TAM side effects and acquired resistance.

In this context, a synthetic strategy exploits the synthesis of new non-steroidal fixed ring structures derived from the stilbene skeleton in the aim to prevent the isomerization that occurs around the double bond in the triphenylethylenes. These structures include benzothiophenes (Raloxifene **4**, SERM **5**),^{16,17} naphthalenes (lasofoxifene **6**, LY 326.315 **7**),¹⁸ benzopyrans (EM 800 **8**, acolbifene **9**)¹⁹ and benzocycloheptenes **10** and **11**²⁰ that cannot isomerize (Fig. 2).

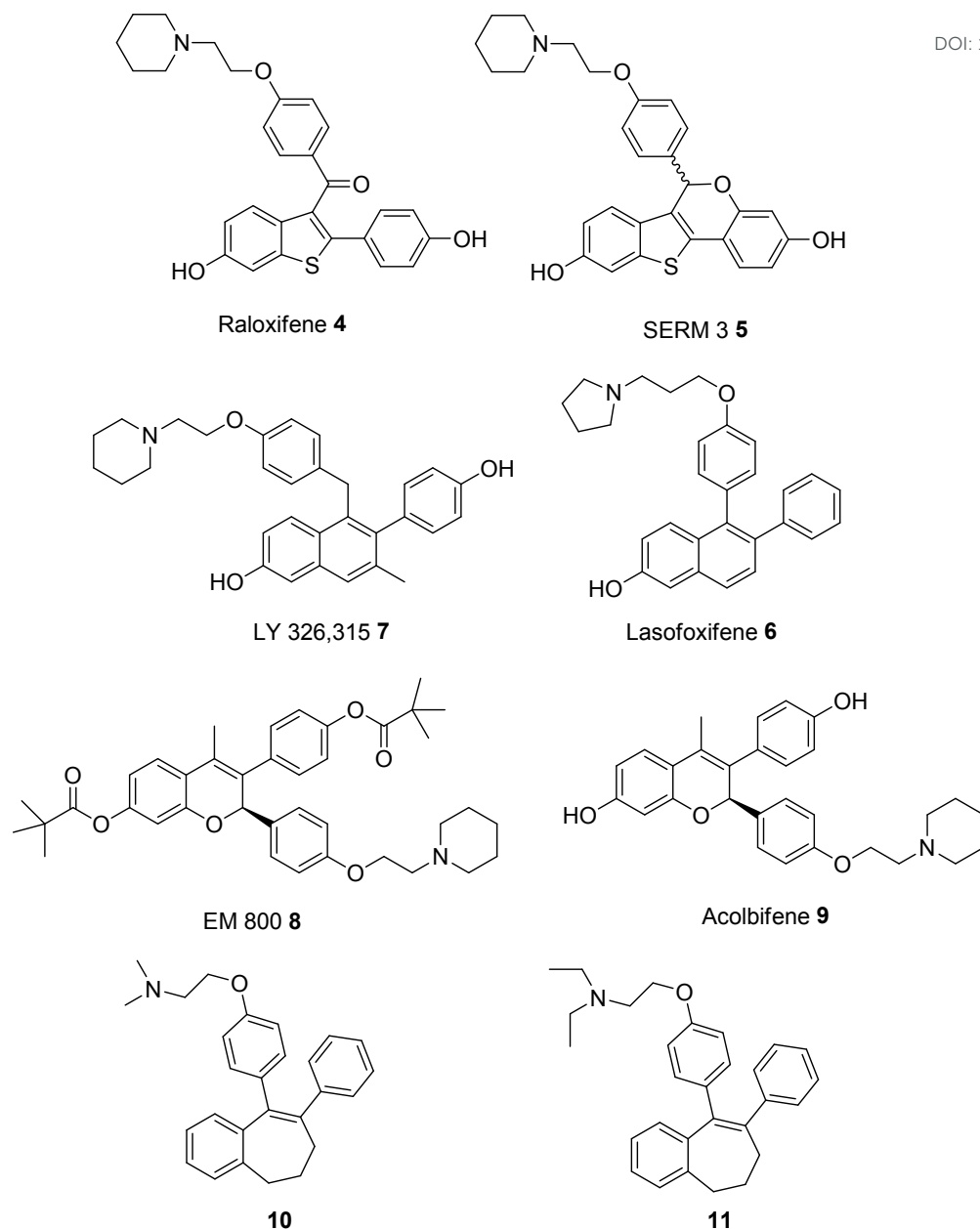


Fig. 2 Non-steroidal fixed ring structures derived from the stilbene skeleton.

According to the same strategy, we wanted to explore if the substitution of the *Z* double bond with a conformationally restricted cyclic C-N bond still keeps the biological features of TAM. Thus, we have synthesized a series of new *cis*-restricted stilbenes **14** (Fig. 3), characterized by the presence of an 1,2,4-oxadiazole-5-one system, where the C=C double bond has been replaced by a *cis* locked C-N bond, as a potential anti-breast cancer agents. The choice of 1,2,4-oxadiazole unit as linker of the two aromatic rings of stilbenes arises from the consideration that this heterocyclic nucleus itself shows anticancer activity in different cancer cell lines.²¹

The new synthesized compounds were subsequently screened in MCF-7 cancer cell line, evaluating their effect on cellular viability. The most active compounds were assessed on the expression levels

of p53 and the ability to activate the apoptotic pathway by testing caspase-3 cleavage was detected. The effect of the compounds was also compared with normal human fibroblast primary cell cultures (HLF), using TAM as drug control. Furthermore, molecular docking studies were assessed in order to investigate the binding affinity of the synthesized compounds to ER α .

2. Results and discussion

The synthetic approach leading to the formation of the differently substituted 1,2,4-oxazolidinyl-5-ones **14a-k** is based on the 1,3-dipolar cycloaddition of nitrones **12a-f** to isocyanates **13a-d** as dipolarophiles (Fig. 3). Nitrones **12a-f**, obtained by reaction of the corresponding aldehydes with *N*-methyl or *N*-aryl hydroxylamine,²² were reacted with isocyanate **13a-d** at room temperature in dichloromethane dry (or dry acetone) and in nitrogen atmosphere for 24 h, leading to cycloadducts **14a-k** in good yields (58-98%) (Table 1). Lower yields were observed for entries 4-6 underlying the pivotal role of the substituent present at the nitrogen atom of the nitron moiety in the control of cycloaddition process efficiency (Table 1). In particular, the presence of the 4-MeO-C₆H₄-CH₂-group onto nitron moiety (R¹) increases the nucleophilicity of **12c**, favoring the formation of by-products and reducing the yields of the desired cycloadducts **14d-f**.

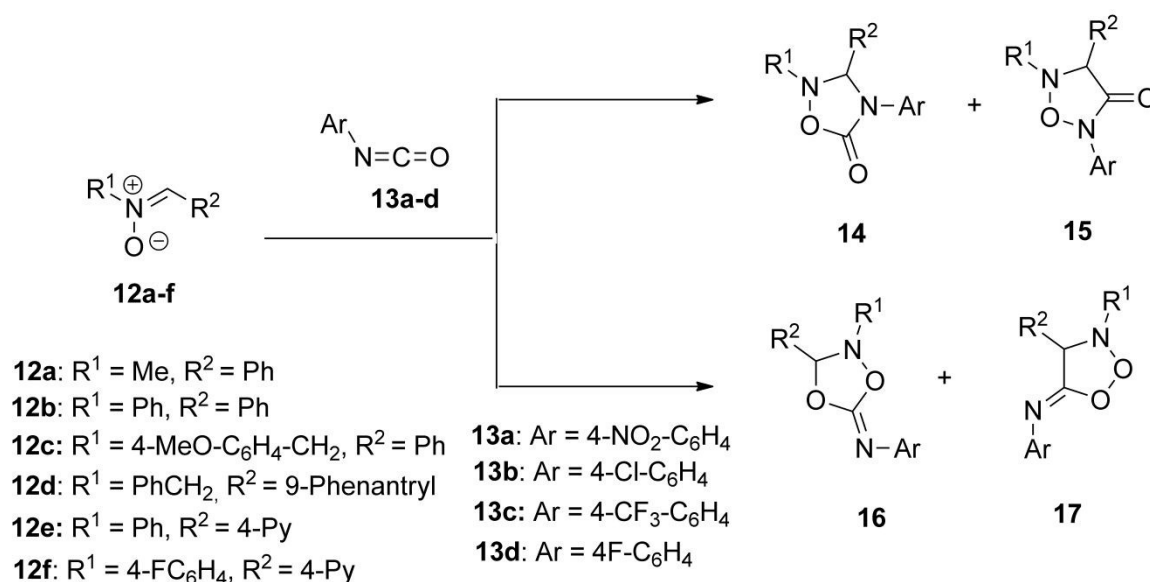
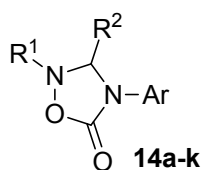


Fig. 3 Reaction of nitrones **12a-f** with isocyanates **13a-d**.

Table 1. Synthesis of 1,2,4-oxazolidinyl-5-ones **14a-k** by 1,3-dipolar cycloaddition.View Article Online
DOI: 10.1039/C9OB00651F

Entry	R ¹	R ²	Ar	Product (yield (%)) ^a
1	Me	Ph	4-NO ₂ -C ₆ H ₄	14a (70%)
2	Ph	Ph	4-NO ₂ -C ₆ H ₄	14b (85%)
3	Ph	Ph	4-Cl-C ₆ H ₄	14c (98%)
4	4-MeO-C ₆ H ₄ -CH ₂	Ph	4-NO ₂ -C ₆ H ₄	14d (68%)
5	4-MeO-C ₆ H ₄ -CH ₂	Ph	4-Cl-C ₆ H ₄	14e (58%)
6	4-MeO-C ₆ H ₄ -CH ₂	Ph	4-CF ₃ -C ₆ H ₄	14f (71%)
7	Ph-CH ₂	9-Phenanthryl	4-NO ₂ -C ₆ H ₄	14g (81%)
8	Ph-CH ₂	9-Phenanthryl	4-Cl-C ₆ H ₄	14h (79%)
9	Ph	4-Py	4-NO ₂ -C ₆ H ₄	14i (76%)
10	Ph	4-Py	4-F-C ₆ H ₄	14j (77%)
11	4-F-C ₆ H ₄	4-Py	4-NO ₂ -C ₆ H ₄	14k (83%)

^a Isolated yields.

The structure of the obtained adducts has been assigned on the basis of spectroscopic data. In particular, the ¹H NMR spectra of the synthesized compounds show the presence of the diagnostic methine proton at C-3, which is located in the range 5.80-6.10 ppm, typical of a NCH(R)N system, as in compounds **14**. In the alternative regioisomers **15**, the methine proton at C-2 should resonate at higher fields as a consequence of O=CCH(R)N structure that involves an higher charge density on these protons according to a reduced electronegative effect of the carbon respect to nitrogen one.

Similar trends have been obtained for the ¹³C of methine carbons of adducts **14** that fall to δ values between 77.5-86.9 ppm. ¹³C spectra of methine carbons for compounds **15** is expected to occur between 67-70 ppm. As a further support to the assigned structure, the presence in the MS spectra of the diagnostic peak at M⁺ -44, resulting from the loss of CO₂ from the molecular ion, is only amenable towards cycloadducts **14**. Furthermore, the isomers **16** and **17**, obtainable from a alternative site selectivity of the nitrene **12** on the double C=O bond of isocyanate **13**, should not present these values of chemical shift. In particular the ¹H NMR spectra of CH proton of compounds **16** should resonate at 5.0-4.9 ppm according to a CHNO assemblage, while the same signal into compounds **17** should resonate at lower fields and in the range between 6.7-6.5 δ, due to OCHN structure.

The obtained results indicate that the reaction proceeds with complete site- and regioselectivity leading to only 1,2,4-oxadiazolidin-5-ones **14a-k** with no traces of the alternative cycloadducts **15-17** (Fig. 3).

Theoretical calculations

The observed site- and regioselectivity of the 1,3-dipolar cycloaddition process have been rationalized using the Truhlar's functional at the M06-2X²³ level of theory with cc-pVTZ basis set.

The modeling study was performed on the reaction between nitrene **12b** and isocyanate **13a**.

In theory, four different approaches were expected to yield cycloadducts **14b-17b**. In fact, the nitrene **12b** might attack the C=N site of isocyanate with a regioselectivity O1(**1b**)-C2(**2b**)/ C3(**1b**)-N1(**2b**) giving **14b** or O1(**1b**)-N1(**2b**)/ C3(**1b**)-C2(**2b**) with the obtainment of **15b** or the C=O site with the alternative regioselectivity O1(**1b**)-C2(**2b**)/ C3(**1b**)-O(**2b**) and O1(**1b**)-O(**2b**)/ C3(**1b**)-C2(**2b**) that gives **16b** and **17b**, respectively. Experimentally, only compound **14b** was obtained.

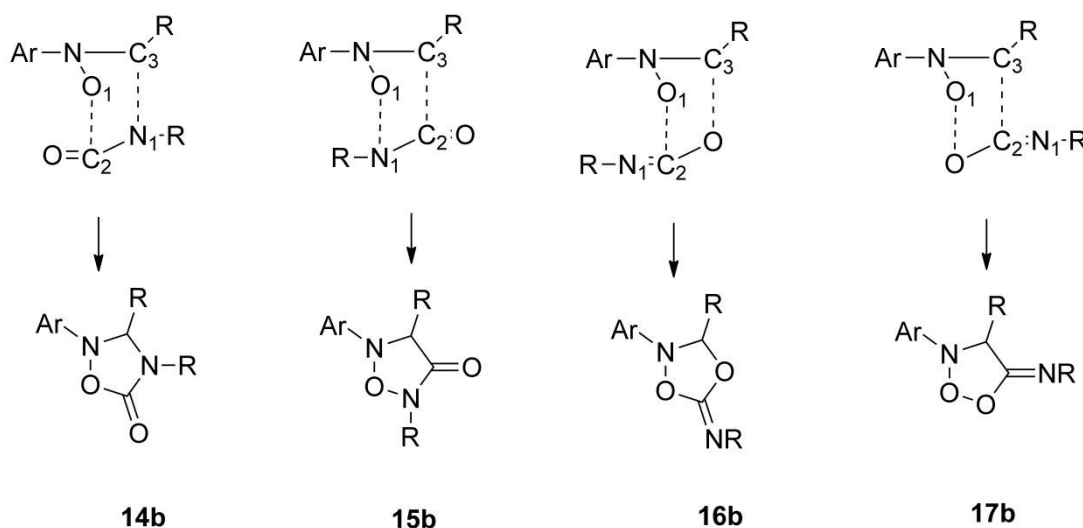


Fig. 4 Expected cycloadducts from reaction of **12b** with **13a**.

In order to rationalize the regioselectivity of the reaction, firstly, the reagents were optimized and the electronic effects taken under consideration.²⁴ Considering the HOMO-LUMO relative position, the dominant electronic interaction involves the HOMO of the dipole and the LUMO of the dipolarophile (ΔE HOMO**12b**-LUMO**13a** < ΔE HOMO**13a**-LUMO**12b**); so it is evident that the reaction is HOMO-controlled dipole (Fig. 5).

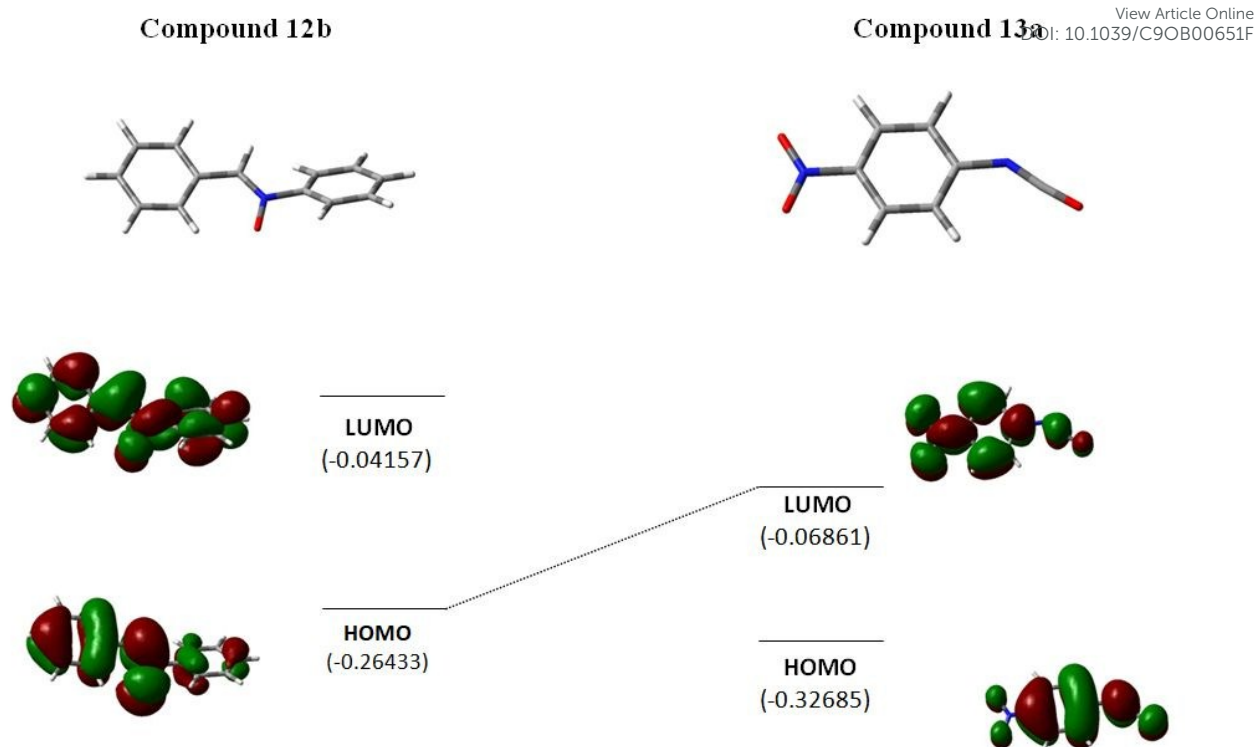


Fig. 5 3D-plots of the frontier molecular orbitals (HOMO and LUMO) of reagents **12b** and **13a**.

In Table 2 the energy values of the HOMO and LUMO orbitals, the electrophilicity index ω ,²⁵ and the nucleophilicity index N ²⁶ of compounds **12b** and **13a** are reported.

Table 2. Computed data of the minimum energy conformation of **12b** and **13a**.

	E_{homo} (eV)	E_{lumo} (eV)	ω	N
12b	-7.14	-1.04	1.37	4.02
13a	-8.86	-1.76	1.98	2.31

The electrophilicity ω value for **13a** is 1.98 eV, corresponding to strong electrophiles. Nitron **12b** presents a lower ω value (1.37 eV), still in the range of moderate electrophiles. On the other hand, **12b** shows a high nucleophilicity index N of 4.02 eV, typical of strong nucleophiles, while isocyanate **13a**, showing N of 2.30 eV is a very moderate nucleophile. So, on the basis of the calculated indices, it is possible to assert that in this cycloaddition the nitron **12b** is the nucleophile, and isocyanate **13a** is the electrophile.

Once the nucleophile and the electrophile of the reaction have been identified, we proceeded to rationalize the regioselectivity of the reaction considering that, in a polar cycloaddition between non-symmetrical compounds, the most favorable interaction involves the most nucleophilic center of the nucleophile and the most electrophilic center of the electrophile.²⁶ As well known, Parr functions are very useful, in order to determine the local reactivity. So, the following step was to

calculate nucleophilic \mathbf{Pk}^- Parr functions for nitrone **12b** and electrophilic \mathbf{Pk}^+ Parr function for isocyanate **13a**.²⁷ The calculated values are reported in **Table 3**.

View Article Online
DOI: 10.1039/C9OB00651F

Table 3. Values of nucleophilic \mathbf{Pk}^- Parr functions for nitrone **12b** and electrophilic \mathbf{Pk}^+ Parr function for isocyanate **13a**.

12b		13a	
	\mathbf{Pk}^-		\mathbf{Pk}^+
\mathbf{Pk}^+		\mathbf{Pk}^+	
\mathbf{N}_2	0.029	\mathbf{N}_1	-0.045
\mathbf{O}_1	0.526	\mathbf{C}_2	0.063
\mathbf{C}_3	0.136	\mathbf{O}_3	0.029

In the case of nitrone **12b**, considering the nucleophilic \mathbf{Pk}^- Parr function values, \mathbf{O}_1 is the most nucleophilically activated center. The electrophilic \mathbf{Pk}^+ Parr functions for isocyanate **13a** indicate that \mathbf{C}_2 is the most electrophilic center. Consequently, the most favorable electrophile-nucleophile interaction along the reaction takes place between \mathbf{O}_1 atom of **12b** and \mathbf{C}_2 atom of **13a**. The reaction could be considered completely regioselective, with the possibility to obtain only derivatives **14b** and **16b**.

Then, in order to determine the site-selectivity of the reaction, and to support the obtained cycloadducts, starting by data reported by Merino *et al.*,²⁸ the transition states leading to **14b**, **15b**, **16b** and **17b** were constructed and located. Optimizations were performed in *vacuo* at the M06-2X/cc-pVTZ level,²⁹ as reported in literature.³⁰

In Fig. 6 are shown the 3-D plots of the four transition states **TS3**, **TS4**, **TS5**, and **TS6** for the different reaction channels, with the forming bonds distances reported (Å).

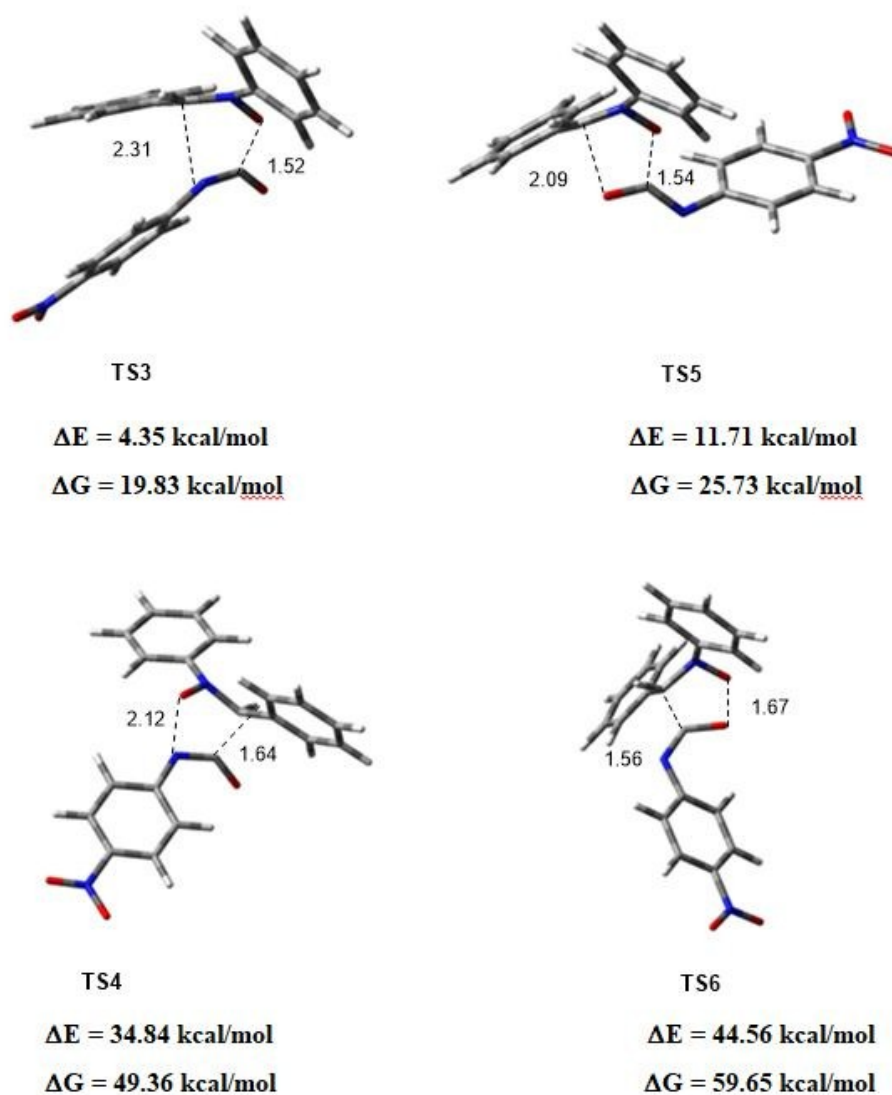


Fig. 6 3-D plots of the four preferred transition states **TS3**, **TS5** and **TS4**, **TS6** leading to expected cycloadducts **14b**, **15b**, **16b** and **17b**. The forming bonds distances are reported in Å.

The IRC analysis allowed to verify that the reaction is concerted, albeit asynchronous as evident by the bond distances. The transition state **TS3** is favorite ($\Delta G= 19.83$ kcal/mol; $\Delta E= 4.35$ kcal/mol; 99% (408 K)) with respect to **TS5** ($\Delta G= 25.73$ kcal/mol; $\Delta E= 11.71$ kcal/mol; 1% (408 K)) and in particular to respect to **TS4** ($\Delta G= 49.36$ kcal/mol; $\Delta E= 34.84$ kcal/mol) and **TS6** ($\Delta G= 59.65$ kcal/mol; $\Delta E= 44.56$ kcal/mol) that are too high to be reached. So, computational data showed a total site-selectivity with the exclusive obtainment of product **14b**.

In conclusion, the modeling study, according to the experimental results, rationalized that the 1,3-dipolar cycloaddition of **12b** and **13a** is regio- and site-selective.

BIOLOGICAL RESULTS

Cellular viability

To monitor cell viability MTT assays were used. MCF-7 cancer cell line and HLF primary cell cultures were exposed to different concentrations (0.5–100 μM) of the tested compounds for 24 h. In parallel, a group of cell cultures was treated with 10 μM of TAM for 24 h. The concentration of compound required to cause 50% inhibition of cell proliferation (IC_{50}) was calculated from concentration–effect curves using Prism 5.0 (GrafPAD Software for Science) and a non-linear regression analysis was used (Tab. 4).

The compounds **14d-f**, **14h** and **14k** showed a significant degree of cytotoxic on the MCF-7 cell line, showing a range of activity of IC_{50} between 15.63 and 31.82 μM . The most active compound was **14d** that showed an IC_{50} value of 15.63 μM . In contrast, the other compounds **14a-c**, **14g**, **14i**, and **14j** displayed a low level of cytotoxicity having a range between 80.23 and 85.34 μM . The exposure of MCF-7 cell line to 10 μM of TAM for 24 h induced a significant decrease of cellular viability ($\text{IC}_{50} = 10.38 \mu\text{M}$). A low decrease in cellular viability in HLF cells, exposed for 24 h, when were treated with 10 μM TAM or with the synthesized compounds at all concentrations was observed.

Table 4. Concentrations (μM) of investigated compounds **14a–14k** that induces for 24 h 50% inhibition of cell proliferation (IC_{50}) in MCF-7 human cancer cell line and HLF primary cell cultures.

Compound	HLF	MCF-7
Untreated (control)	>100	>100
Tamoxifen	82.14 \pm 0.23	10.38 \pm 0.09*
14a	80.75 \pm 0.32	85.34 \pm 0.22
14b	81.23 \pm 0.19	83.64 \pm 0.17
14c	80.91 \pm 0.21	80.23 \pm 0.33
14d	82.01 \pm 0.48	15.63 \pm 0.26*
14e	81.23 \pm 0.15	22.76 \pm 0.08*
14f	81.93 \pm 0.12	26.14 \pm 0.21*
14g	82.36 \pm 0.24	83.62 \pm 0.22
14h	81.99 \pm 0.11	17.80 \pm 0.13*
14i	81.22 \pm 0.27	80.97 \pm 0.34
14j	81.48 \pm 0.39	80.64 \pm 0.28
14k	81.22 \pm 0.31	31.82 \pm 0.24*

Each data represents the mean \pm SD from for independent experiments performed in triplicate. Tamoxifen (10 μM) was uses as positive control. Values represent the mean \pm S.D. of four experiments performed in triplicate. * $p < 0.001$ vs control.

Effect of the most active compounds (14d, 14h, 14e, 14f and 14k) on p53 expression levelsView Article Online
DOI: 10.1039/C9OB00651F

Figure 7 shows representative immunoblots (Fig. 7A) and densitometric analysis (Fig. 7B) of p53 expression levels in total cell lysates from MCF-7 cell lines exposed to 10 μ M **14d**, **14h**, **14e**, **14f**, **14k** or TAM for 24 h. The treatment of the cells with these compounds led to a significant increase of p53 protein expression levels, when compared with the untreated cells used as a control. The effect appeared more evident when the cells were exposed to the compounds **14d**, **14h**, **14e** and **14f**. Compound **14k** showed a lower increase in p53 expression levels, when compared with the other compounds. However, the levels of p53 expression were lower than observed in TAM exposed cells.

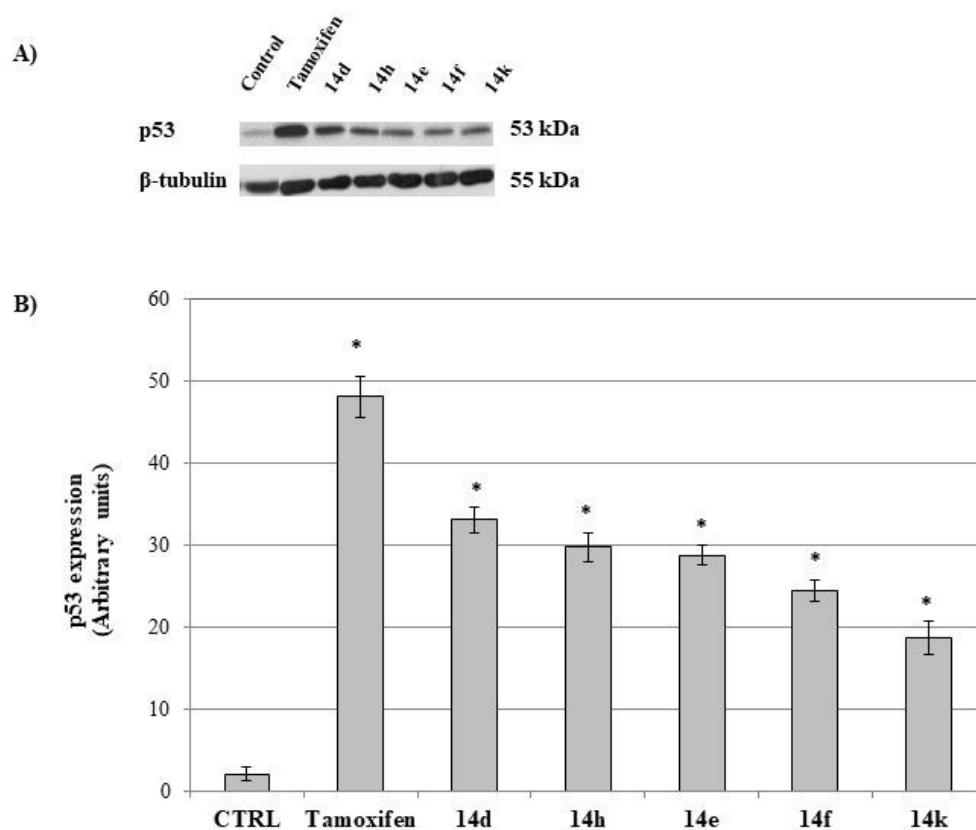


Fig. 7: A) Representative Western blots and B) semiquantitative analyses of p53 expression levels evaluated in total cell lysates from MCF-7 cell line unexposed (control) or exposed for 24 h to 10 μ M **14d**, **14h**, **14e**, **14f**, **14k**. Tamoxifen was used as drug control. Levels of protein were normalized with β -tubulin. Values represent the mean \pm S.D. of four separated experiments performed in triplicate. * $p < 0.001$ vs control.

Effect of the most active compounds (**14d**, **14h**, **14e**, **14f** and **14k**) on caspase-3 cleavage

View Article Online
DOI: 10.1039/C9OB00651F

To elucidate whether **14d**, **14h**, **14e**, **14f** and **14k** were able to activate the apoptotic pathway, caspase-3 cleavage through Western Blot analysis was assessed (Fig. 8). Compounds **14d**, **14h**, **14e**, **14f** and **14k** induced a significant increase of caspase-3 cleavage, when compared with the control. The effect appeared more evident in **14d**, **14h**, **14e** and **14f** exposed cells, even if it appeared lower than found cells treated with tamoxifen. Compound **14k** was also able to activate caspase-3 cleavage but at lower levels than the other compounds.

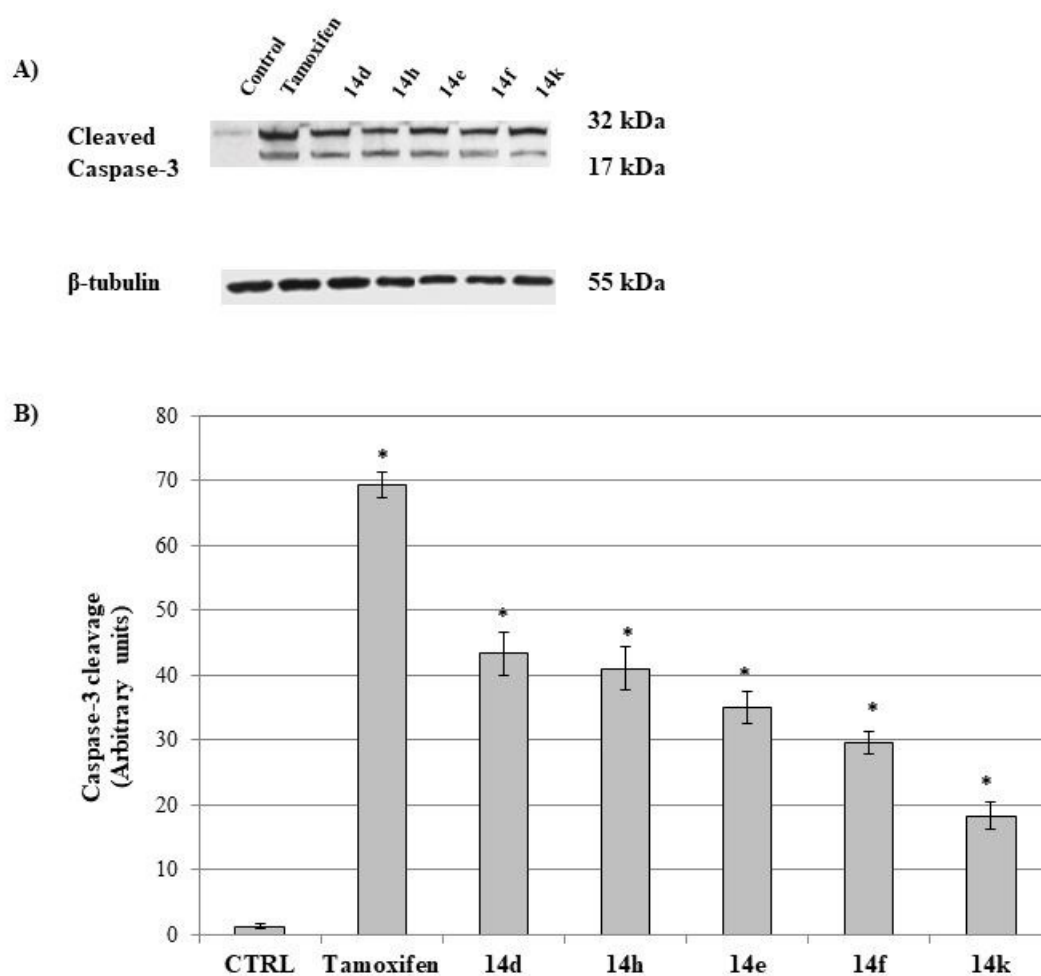


Fig. 8: A) Representative Western blots and B) semiquantitative analyses of caspase-3 cleavage evaluated in total cell lysates from MCF-7 cell line unexposed (control) or exposed for 24 h to 10 μ M **14d**, **14h**, **14e**, **14f**, **14k**. Tamoxifen was used as drug control. Cleaved caspase-3 levels were normalized with β -tubulin. Values are the mean \pm S.D. of four separated experiments performed in triplicate. * $p < 0.001$ vs control.

Molecular modeling study

To explain the different activity of the novel compounds, a computational docking study was undertaken for compounds **14a-k**. The crystal structure of ER α in complex with 4-OH-TAM (PDB code: 3ERT) was selected based on a good experimental resolution (1.9 Å). The accuracy of the docking protocol was validated by re-docking method of 4-OH-TAM in the binding site to determine the lowest RMSD relative to the crystallographic pose. 4-OH-TAM was successfully re-docked with a RMSD of 1.02 Å. The ER α has ligand-binding domain (LBD) which is predominantly the hydrophobic cavity that composed by amino acid residues from helices 3, 6, 7, 8, 11, and 12. The agonist and antagonist activity of a ligand is determined by the helix-12 from residues 536-544 in its macromolecule (ER α). When an antagonist for example 4-OHT binds to LBD of ER α , the helix-12 will be closed and not binds to co-activator so it has the antagonist activity based on the absence of hydrogen bond interaction with His524.³² Thus, the selective binding of the potential anti-breast cancer agents will rely largely on contributions from hydrophobic interactions. The docking of compounds **14a-k** revealed a strong presence of hydrophobic interactions and in a similar fashion as does 4-OH-TAM, nine out of eleven derivatives, establish hydrogen bond with Arg394. Docking results are summarized in Table 5.

Table 5. Results of molecular docking of **14a-k** in ligand binding domain of estrogen receptor alpha (ER α)

Compound	ΔG Kcal/mol	Calculated Ki (nM)	Number in Cluster	Interactions with Amino Acids			
				Hydrogen Bond	van der Waals (Hydrophobic)		
14a	-8.33	789.90	100	Arg394, O (NO ₂)	Met343, Trp383, Leu387, Leu391, Leu525	Leu346, Leu384, Leu391, Leu525	Ala350, Met388,
14b	-9.77	68.43	100	-	Met343, Ala350, Met421, Ile424, Leu525,	Leu346, Met388, Leu391,	Thr347, Leu391,
14c	-8.85	325.69	100	Arg394, Cl	Met343, Leu349, Leu387, Met421, Ile424, Leu525,	Leu346, Ala350, Leu391,	Thr347, Trp383, Phe404,
14d	-10.70	14.47	51	Arg394, O (OCH ₃)	Met343,	Leu346,	Thr347,

					Ala350, Leu387, Met388, Leu391, Phe404, Met421, Ile424, Leu525
14e	-9.53	103.70	43	Arg394, O (OCH ₃)	Met343, Leu346, Thr347, Ala350, Leu387, Met388, Leu391, Phe404, Met421, Ile424, Leu525, Met528
14f	-9.16	192.83	37	Arg394, O (OCH ₃) Thr347, F (CF ₃)	Met343, Leu346, Ala350, Leu387, Met388, Leu391, Phe404, Met421, Ile424, Leu525, Met528
14g	-10.04	43.36	34	-	Met343, Leu346, Thr347, Leu349, Ala350, Trp383, Leu384, Leu387, Leu391, Phe404, Ile424, Leu525, Met528,
14h	-10.64	15.77	47	Arg394, O (NO ₂)	Met343, Leu346, Thr347, Ala350, Trp383, Leu387, Met388, Met421, Ile424, Leu525, Met528
14i	-9.85	60.27	100	-	Met343, Leu346, Ala350, Trp383, Leu384, Leu387, Met388, Leu391, Met421, Leu525
14j	-8.55	537.92	100	Arg394, F	Met343, Leu346, Leu349, Ala350, Leu384, Leu387, Met388, Phe404, Met421, Ile424, Leu525
14k	-8.93	296.10	84	Arg394, F	Met343, Ala350, Trp383, Leu384, Leu387, Met388, Leu391, Met421, Ile424, Leu525
4-OH-TAM	-11.48	3.85	100	Glu353, Arg394	Met343, Leu346, Leu349, Ala350, Trp383, Leu384, Leu387, Met388, Leu391, Phe404, Met421, Ile424, Leu428, Leu525,

View Article Online
DOI: 10.1039/C9OB00651F

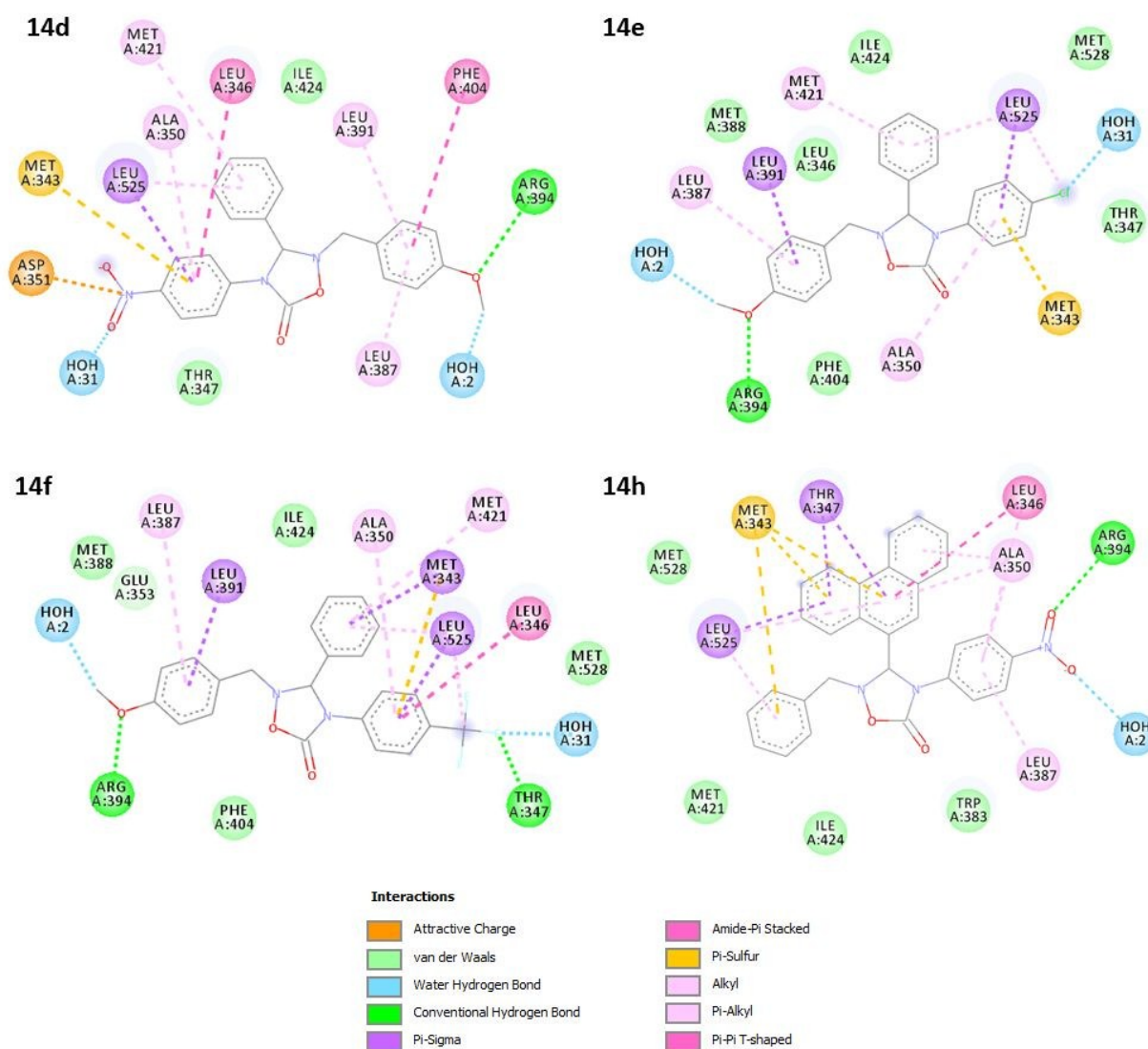


Fig. 9 2D interactions of compounds **14d**, **14e**, **14f** and **14h** in the estrogen receptor- α ligand binding domain.

Compounds **14a-k** shared a similar interaction constituting an extensive hydrophobic network and in addition compounds **14a**, **14c-f**, **14h** and **14j-k** showed hydrogen bond with Arg394. The best docking pose of the most active compounds (**14d**, **14e**, **14f**, **14h**) were analyzed to highlight important binding interaction of the drug candidates as anticancer agents. Compounds **14d**, **14e**, **14f** and **14h** revealed a strong presence of hydrophobic interactions between Met343, Leu346, Ala350, Leu387, Met388, Leu391, Met421, Ile424 and Leu525 with the aromatic rings of the ligands. Compounds **14d**, **14f** and **14h** presented an additional hydrophobic interaction with Thr347 and the compounds **14e** and **14f** showed two additional hydrophobic bonds with Phe404 and Met528, while compound **14h** differed by van der Waals interaction with Trp383 as well as the compound **14d**

formed a unique T-shaped π -stacking interaction with Phe404. Each ligand showed hydrogen bond with Arg394, similar to the 4-OH-TAM. Compounds **14d**, **14e** and **14f** formed direct hydrogen bond between the hydrogen bond donor Arg394 and the oxygen of the methoxy group, while compound **14h** established hydrogen bond between the hydrogen bond donor Arg394 and the oxygen of nitro group. Moreover, compound **14f** established an additional hydrogen bond with Thr347 by a fluorine of the CF₃ group. Additionally, compound **14d**, the most active compound, interact with the negatively charged residue Asp351 in the ligand binding domain of the ER by a nitro group, suggesting that Asp351 plays a key role in antagonist binding.

5. Conclusion

A series of 3,4-diaryl-1,2,4-oxadiazolidin-5-ones, synthesized by 1,3-dipolar cycloaddition of nitrones to isocyanates as fixed-ring analogues of TAM, a drug inhibitor of ER used in breast cancer therapy, have been reported. The structure of the obtained adducts was investigated on the basis of spectroscopic data. The observed site- and regioselectivity of the 1,3-dipolar cycloaddition processes was rationalized by theoretical calculations using the Truhlar's functional at the M06-2X level of theory. Some of new synthesized compounds (**14d-f**, **14h** and **14k**) showed a significant cytotoxic effect in MCF-7 human breast cancer cell line. In addition, compounds **14d-f**, **14h** and **14k** were able to increase the p53 expression levels, activating also the apoptotic pathway, when compared with the control. Molecular modeling studies of novel compounds, performed on the crystal structure of ER, reveal the presence of strong hydrophobic interactions with the aromatic rings of the ligands similar to TAM. The obtained results suggest that the 1,2,4-oxadiazolidin-5-one ring system can replace the structurally more simple double bond present in TAM, and that the effect of the compounds **14d-f**, **14h** and **14k** in MCF-7 breast cancer cell line might due partially *via* the inhibition of the ER. However, further studies are needed to better clarify the role played by the new synthesized compounds in MCF-7 cancer cell line as inhibitor of ER. In addition, the effect of the most active compound (**14h**) in breast cancer animal model will be the object of future biological studies. The results reported in this study represent a starting point for future SAR and docking studies to find new TAM analogues with a better pharmacological profile.

Experimental section

Materials and methods

Solvents and reagents are commercial. ESI-HRMS were determined with a Thermo Fischer Scientific LTQ Orbitrap XL. NMR spectra (¹H NMR at 500 MHz, ¹³C NMR at 126 MHz) were recorded with Varian instruments and are reported in ppm relative to CDCl₃ (7.26, and 77.0 ppm

respectively). Furthermore, ^{13}C NMR spectra were recorded using the Attached Proton Test (APT) View Article Online
DOI: 10.1039/C9OB00651F technic. Merck silica gel 60-F254 precoated aluminum plates have been used for thin-layer chromatographic separations. Flash chromatography was performed on Merck silica gel (200–400 mesh). Preparative separations were carried out by a MPLC Büchi C-601 by using Merck silica gel 0.040–0.063 mm. All compounds were determined to have purity >95% using Shimadzu LC/MS/MS-8040 system (C18 column; eluting gradient 10-90% acetonitrile in water).

General procedure.

1.1 To nitrone **12** (1 mmol) in dichloromethane or acetone dry (5 ml) at room temperature, is added the corresponding aryl isocyanate **13** (1 mmol). The solution is stirred at rt for 24 h and then concentrated in *vacuo* to afford a yellow solid which was triturated with 10 ml of methanol for 3 h. The resulting suspension was filtered off, and the solid was washed with hexane and then purified by silica gel column chromatography to yield final desired compounds **14a-k**.

2.1. 2-methyl-4-(4-nitrophenyl)-3-phenyl-1,2,4-oxadiazolidin-5-one (**14a**). Eluent cyclohexane/ethyl acetate 9:1; yellow solid (yield 70%); mp = 107-110 °C. ν_{max} / cm^{-1} : 1746 (C=O). ^1H NMR (500 MHz, CDCl_3): δ 8.14 (d, J = 9.0 Hz, 2H), 7.53 (d, J = 9.0 Hz, 2H), 7.40–7.42 (m 5 H), 5.72 (s, 1H), 3.06 (s, 3H). ^{13}C NMR (125 MHz, CDCl_3): δ 153.8, 143.9, 142.0, 139.2, 131.8, 130.5, 129.4, 127.1, 124.8, 119.5, 85.0, 53.0. HRMS-EI (M/z) calcd for $\text{C}_{15}\text{H}_{13}\text{N}_3\text{O}_4$ 299.0906 found 299.0901.

2.2 4-(nitrophenyl)-2,3-diphenyl-1,2,4-oxadiazolidin-5-one (**14b**). Eluent cyclohexane/ethyl acetate 9:1; yellow solid (yield 85%); mp = 125-128 °C. ν_{max} / cm^{-1} : 1765 (C=O). ^1H NMR (500 MHz, CDCl_3): δ 8.15 (d, J = 8.5 Hz, 2H), 7.56 (d, J = 8.50 Hz, 2H), 7.47–7.42 (m, 5H), 7.43-7.40 (m, 2H), 7.26-7.25 (m, 3H), 6.23 (s, 1H). ^{13}C NMR (125 MHz, CDCl_3): δ 153.8, 148.8, 146.3, 141.4, 134.5, 130.5, 129.6, 127.0, 124.9, 119.3, 117.5, 85.9. HRMS-EI (M/z) calcd for $\text{C}_{21}\text{H}_{16}\text{N}_2\text{O}_4$ 360.1110 found 360.0999.

2.3. 4-(4-chlorophenyl)-2,3-diphenyl-1,2,4-oxadiazolidin-5-one (**14c**). Eluent cyclohexane/ethyl acetate 8:2; white solid (yield 98%); mp = 120-122 °C. ν_{max} / cm^{-1} : 1754 (C=O). ^1H NMR (200 MHz, CDCl_3): δ 7.49-7.48 (m, 2H), 7.44-7.43 (m, 3), 7.41-7.38 (m, 2H), 7.24-7.21 (m, 7), 6.10 (s, 1H). ^{13}C NMR (125 MHz, CDCl_3): δ 154.1, 149.2, 135.3, 134.2, 130.3, 129.5, 129.4, 129.3, 128.1, 127.2, 125.9, 122.4, 117.8, 86.5. HRMS-EI (M/z) calcd for $\text{C}_{20}\text{H}_{15}\text{ClN}_2\text{O}_2$ 350.0822 found 350.0829.

2.4. 2-(4-methoxybenzyl)-4-(4-nitrophenyl)-3-phenyl-1,2,4-oxadiazolidin-5-one (**14d**). Eluent cyclohexane/ethyl acetate 4:1, yellow solid (yield 68%); mp = 129-132 °C. ν_{max} / cm^{-1} : 1747 (C=O). ^1H NMR (500 MHz, CDCl_3): δ 8.14 (d, J = 9.0 Hz, 2H), 7.51 (d, J = 9.0 Hz, 2H), 7.37-7.30 (m, 5H), 7.16 (d, J = 8.0 Hz, 2H), 6.91 (d, J = 8.0 Hz, 2H), 5.87 (s, 1H), 4.42 (d, J = 14 Hz, 1 H), 4.14 (d, J = 14 Hz, 1 H), 3.82 (s, 3H). ^{13}C NMR (125 MHz, CDCl_3): δ 160.0, 154.3, 142.8, 142.0, 134.3, 131.1, 130.1, 129.3, 126.5, 124.9, 124.8, 118.6, 114.4, 79.9, 62.0, 55.3. HRMS-EI (M/z) calcd for $\text{C}_{22}\text{H}_{19}\text{N}_3\text{O}_5$ 405.1325 found 405.1330.

2.5. 4-(4-chlorophenyl)-2-(4-methoxybenzyl)-3-phenyl-1,2,4-oxadiazolidin-5-one (**14e**). Eluent cyclohexane/ethyl acetate 9:1; pale yellow solid (yield 58%); mp = 100-103 °C. $\nu_{\text{max}}/\text{cm}^{-1}$: 1739 (C=O). $^1\text{H NMR}$ (500 MHz, CDCl_3): δ 7.34-7.15 (m, 11H), 6.89 (d, $J = 8.8$ Hz, 2H), 5.74 (s, 1H), 4.38 (d, $J = 12.8$ Hz, 1H), 4.14 (d, $J = 12.8$ Hz, 1H), 3.79 (s, 3H). $^{13}\text{C NMR}$ (125 MHz, CDCl_3): δ 159.9, 151.6, 134.9, 131.1, 130.6, 130.5, 129.7, 129.6, 126.8, 126.1, 125.3, 121.2, 114.3, 80.5, 61.8, 55.3. HRMS-EI (M/z) calcd for $\text{C}_{22}\text{H}_{19}\text{ClN}_2\text{O}_3$ 394.1084 found 394.1100.

2.6. 2-(4-methoxybenzyl)-3-phenyl-4-(4-(trifluoromethyl)phenyl)-1,2,4-oxadiazolidin-5-one (**14f**). Eluent cyclohexane/ethyl acetate 9:1; yellow oil (yield 71%). $\nu_{\text{max}}/\text{cm}^{-1}$: 1728 (C=O). $^1\text{H NMR}$ (500 MHz, CDCl_3): δ 7.51 (d, $J = 8.5$ Hz, 2H), 7.43 (d, $J = 8.5$ Hz, 2H), 7.37-7.28 (m, 5H), 7.21 (d, $J = 8.5$ Hz, 2H), 6.88 (d, $J = 8.5$ Hz, 2H), 5.81 (s, 1H), 4.40 (d, $J = 14$ Hz, 1H), 4.12 (d, $J = 14$ Hz, 1H), 3.79 (s, 3H). $^{13}\text{C NMR}$ (125 MHz, CDCl_3): δ 159.9, 154.6, 139.5, 135.0, 131.1, 129.8, 129.2, 126.7, 126.6, 125.1, 124.9, 122.7, 119.0, 114.4, 80.0, 61.5, 55.3. HRMS-EI (M/z) calcd for $\text{C}_{23}\text{H}_{19}\text{F}_3\text{N}_2\text{O}_3$ 428.1348 found 428.1353.

2.7. 2-benzyl-4-(4-nitrophenyl)-3-(phenanthren-9-yl)-1,2,4-oxadiazolidin-5-one (**14g**). Eluent cyclohexane/ethyl acetate 4:1; beige solid (yield 81%); mp = 196-198 °C cyclohexane/ethyl acetate 4:1. $\nu_{\text{max}}/\text{cm}^{-1}$: 1757 (C=O). $^1\text{H NMR}$ (500 MHz, CDCl_3): δ 8.74 (d, $J = 8.5$ Hz, 1H), 8.63 (d, $J = 8.5$ Hz, 1H), 8.12 (d, $J = 9.0$ Hz, 2H), 7.76 (d, $J = 8.0$ Hz, 1H), 7.68-7.65 (m, 2H), 7.65-7.34 (m, 10H), 7.11 (m, 1H), 6.67 (s, 1H), 4.64 (d, $J = 12$ Hz, 1H), 4.42 (d, $J = 12$ Hz, 1H). $^{13}\text{C NMR}$ (125 MHz, CDCl_3): δ 155.5, 143.8, 142.1, 131.5, 131.0, 130.6, 130.4, 130.3, 129.4, 129.2, 128.7, 128.6, 128.2, 127.2, 126.9, 126.8, 127.3, 125.8, 125.2, 123.8, 122.7, 122.4, 118.1, 77.5, 63.1. HRMS-EI (M/z) calcd for $\text{C}_{29}\text{H}_{21}\text{N}_3\text{O}_4$ 475.1532 found 475.1530.

2.8. 2-benzyl-4-(4-chlorophenyl)-3-(phenanthren-9-yl)-1,2,4-oxadiazolidin-5-one (**14h**). Eluent cyclohexane/ethyl acetate 4:1; orange solid (yield 79%); mp = 132-136 °C. $\nu_{\text{max}}/\text{cm}^{-1}$: 1752 (C=O). $^1\text{H NMR}$ (500 MHz, CDCl_3): δ 8.71 (d, $J = 8.0$ Hz, 1H), 8.61 (d, $J = 8.0$ Hz, 1H), 7.77 (d, $J = 7.5$ Hz, 1H), 7.67-7.64 (m, 3H), 7.61-7.56 (m, 1H), 7.53-7.41 (m, 6H), 7.33 (d, $J = 10$ Hz, 2H), 7.21 (d, $J = 8.5$, 2H), 7.14-7.08 (m, 1H), 6.55 (s, 1H), 4.59 (d, $J = 12$ Hz, 1H), 4.38 (d, $J = 12$ Hz, 1H). $^{13}\text{C NMR}$ (125 MHz, CDCl_3): δ 157.2, 135.2, 133.2, 131.4, 131.0, 130.8, 130.6, 130.4, 129.8, 129.4, 129.0, 128.6, 127.9, 127.4, 127.1, 126.9, 126.8, 123.0, 122.7, 122.4, 122.3, 122.2, 120.2, 77.8, 62.9. HRMS-EI (M/z) calcd for $\text{C}_{29}\text{H}_{21}\text{ClN}_2\text{O}_2$ 464.1292 found 464.1290.

2.9. 4-(4-nitrophenyl)-2-phenyl-3-(pyridin-4-yl)-1,2,4-oxadiazolidin-5-one (**14i**). Eluent cyclohexane/ethyl acetate 3:1; yellow sticky oil (yield 76%); $\nu_{\text{max}}/\text{cm}^{-1}$: 1730 (C=O). $^1\text{H NMR}$ (500 MHz, CDCl_3): δ 8.63 (d, $J = 7.0$ Hz, 2H), 8.05 (d, $J = 7.5$ Hz, 2H), 7.47 (d, $J = 7.5$ Hz, 2H), 7.41 (d, $J = 7.0$ Hz, 2H), 7.41-7.40 (m, 3H), 7.25 (d, $J = 8.0$ Hz, 2H), 6.25 (s, 1H). $^{13}\text{C NMR}$ (125 MHz, CDCl_3): δ 153.4, 151.0, 148.3, 143.2, 141.0, 136.8, 129.7, 125.0, 121.5, 121.4, 121.2, 117.4, 83.9. HRMS-EI (M/z) calcd for $\text{C}_{19}\text{H}_{14}\text{N}_4\text{O}_4$ 362.1015 found 362.1019.

2.10. 4-(4-fluorophenyl)-2-phenyl-3-(pyridin-4-yl)-1,2,4-oxadiazolidin-5-one (**14j**). Eluent cyclohexane/ethyl acetate 4:1; yellow sticky oil (yield 77%); $\nu_{\text{max}}/\text{cm}^{-1}$: 1748 (C=O). $^1\text{H NMR}$ (500 MHz, CDCl_3): δ 8.52 (d, $J = 6.3$ Hz, 2H), 7.50-7.48 (m, 2H), 7.43 (d, $J = 8.5$ Hz, 2H), 8-7.37 (m, 2H), 7.23-7.21 (m, 3H), 6.97-6.94 (m, 2), 6.06 (s, 1H). $^{13}\text{C NMR}$ (125 MHz, CDCl_3): δ 160.4 (d, $J_{\text{CF}} = 245.6$ Hz), 154.3, 150.6, 149.2, 135.5, 131.4 (d, $J_{\text{CF}} = 3.4$ Hz), 129.4, 127.3, 125.8 (d), 123.9

(d, $J_{CF} = 8.2$ Hz), 117.3, 116.2 (d, $J_{CF} = 22.7$ Hz), 86.9. HRMS-EI (M/z) calcd for $C_{19}H_{13}FN_4O_4$ 335.1070 found 335.1075. View Article Online
DOI: 10.1039/C9OB0651F

2.11 2-(4-fluorophenyl)-4-(4-nitrophenyl)-3-(pyridin-4-yl)-1,2,4-oxadiazolidin-5-one (**14k**). Eluent cyclohexane/ethyl acetate 3:1; yellow sticky oil (yield 83%). ν_{max}/cm^{-1} : 1740 (C=O). 1H NMR (500 MHz, $CDCl_3$): δ 8.75 (d, $J = 6.0$ Hz, 2H), 8.21 (dd, $J = 2.0$ and 9.0 Hz, 2H), 7.54 (dd, $J = 2.0$ and 9.5 Hz, 2H), 7.38 (d, $J = 6.0$ Hz, 2H), 7.27-7.25 (m, 2H), 7.16-7.12 (m, 2H), 6.18 (s, 1H). ^{13}C NMR (125 MHz, $CDCl_3$) δ 162.3 (d, $J_{CF} = 248.7$ Hz), 153.3, 151.1, 142.9 (d, $J_{CF} = 3.2$ Hz), 140.8, 136.7, 125.2, 123.7, 122.1, 119.2 (d, $J_{CF} = 8.3$ Hz), 116.6 (d, $J_{CF} = 22.7$ Hz), 84.2. HRMS-EI (M/z) calcd for $C_{19}H_{13}FN_4O_4$ 380.0921 found 380.0924.

Computational Methods

All of the calculations were performed in vacuo using the Gaussian09 program package.³⁰ Optimizations were performed with the M06-2X functional in conjunction with cc-pVTZ basis set.²⁹ The reaction pathways were confirmed by IRC analyses performed at the same level of calculation. Vibrational frequencies were computed at the same level of theory to define the optimized structures as minima or transition states, that all present an imaginary frequency corresponding to the forming bonds. The polar nature of the reactions has been evaluated through the analysis of the reactivity indices. The electronic chemical potential (μ), chemical hardness (η), global electrophilicity (ω), and global nucleophilicity (N), were computed at the same level as above. The local electrophilicity and nucleophilicity power were determined by the calculation of Parr functions.

Biological evaluation

Materials

MCF-7 human breast cancer cell line was purchased from Cell Bank Interlab Cell Line Collection (Genova, Italy). Human Lymphatic Fibroblasts (HLF), Basal Medium and Fibroblast Growth Supplement (FGS) were provided by Innoprot (Derio Bizkaia, Spain). Dulbecco's Modified Eagle Medium (DMEM) containing 2 mM GlutaMAX, heat inactivated-Foetal Bovine Serum (FBS, GIBC), streptomycin and penicillin antibiotics, Trypsin-EDTA 0,05% solution, SuperSignal West Pico Plus was from Pierce were from ThermoFisher Scientific (Milan, Italy). Poly-L-lysine (1mg/mL), 3(4,5-dimethyl-thiazol-2-yl)2,5-diphenyl-tetrazolium bromide salts (MTT), Tamoxifen free base, Dimethyl Sulfoxide (DMSO), horseradish peroxidase-conjugated anti-mouse IgG and other analytical chemicals were obtained from Sigma-Aldrich (Milano, Italy). Mouse monoclonal antibody against p53 was from Abcam (Milan, Italy). Mouse monoclonal antibody against caspase-3 was from Becton Dickinson (Milan, Italy). Mouse monoclonal antibody against β -tubulin was from Cell Signaling, EuroClone (Milan, Italy). SuperSignal West Pico Plus was from Pierce (ThermoFisher Scientific, Milan, Italy).

Cell Cultures

MCF7 cells were suspended in DMEM containing 10% (v/v) FBS, 2 mM L-glutamine, 50 μ g/mL, penicillin (50 U/mL), plated in a final density of 2×10^6 cells. HLF primary cells were suspended in Basal Medium containing 10% (v/v) FBS, streptomycin (50 μ g/mL), penicillin (50 U/mL) and 5 mL of FGS added to 500 mL of Basal Medium, and seeded at the density of 5,000 cells/cm² of poly-L-lysine-coated flasks. Cell cultures were then incubated at 37°C in humidified atmosphere containing

5% CO₂ (95%-5%) and the medium was replaced every 2 or 3 days. When the cultures were about 80-85% confluent, cells were trypsinized by 0.05% trypsin and 0.53 mM EDTA at 37°C in humidified atmosphere containing 5% CO₂ for 5 min. Trypsinization was stopped by adding 20% FBS, resuspended and plated in flasks fed with fresh basic complete media. Cells were seeded again at 1:4 density ratio and incubated at 37°C in humidified atmosphere containing 5% CO₂.

Treatment of Cells

MCF-7 and HLF primary cells were placed at the final density of 60x10⁴ cells/well of a 96-multiwell flat-bottomed 200- μ L microplates to assess MTT test or in 75 cm² flasks to perform Western Blot analysis and untreated or treated with different concentrations of all synthesized compounds (0.1, 0.5, 1, 5 μ M) for 24, 48 and 72 h. A group of cell was treated with TAM, a well know ER inhibitor in breast cancer, as control drug was used.

MTT bioassay

To monitor cell viability MTT test bioassay was used. MCF-7 and HLF cell lines were set up 6 x 10⁵ cells per well of a 96-multiwell, flat-bottomed, 200- μ L microplate, and maintained at 37°C in a humidified 5% CO₂/95% air mixture.³³ At the end of treatment time, 20 μ L of 0.5% MTT in (pH 7.4) PBS were added to each microwell. After 2 h of incubation with the reagent, the supernatant was removed and replaced with 100 μ L of DMSO and incubated at 37°C for 1 h. The optical density of each well was measured with a microplate spectrophotometer reader (Titertek Multiskan; Flow Laboratories, Helsinki, Finland) at λ =570 nm. Results were normalized with DMSO control (0.05%) and expressed as a percentage of cell viability inhibition. Interactions of compounds and media were estimated on the basis of the variations between the drug-containing medium and drug-free medium to control for false-positive or false negative results. The half maximal inhibitory concentration (IC₅₀) values were obtained graphically from dose-effect curves using Prism 5.0 (GraphPad Software Inc.).³⁴ We found that for the all cultures the optimal concentration of all synthesized compounds was 10 μ M and the exposure time was 24 h. No significant toxic effect of the compound in HLF cell line cultures was found.

Western Blot Analysis

To identified the expression levels of p53 and caspase-3 cleavage Western Blot Analysis was performed in MCF-7 cell line cultures untreated or treated with the most active compounds (**14d**, **14h**, **14e**, **14f** and **14k**) or TAM at the concentration of 10 μ M for 24h. Briefly, untreated and treated MCF-7 cell line cultures were harvested in cold PBS, collected by centrifugation, and resuspended in a homogenizing buffer with 50 mM Tris-HCl (pH 6.8), 150 mM NaCl, 1 mM EDTA, 0.1 mM phenylmethylsulfonyl fluoride (PMSF; Sigma-Aldrich), and 10 μ g/ml of aprotinin, leupeptin, and pepstatin and sonicated on ice.^{33, 35, 36} The protein concentration of the homogenates was then diluted to 1 mg/ml with reducing stop buffer (0.25 M Tris-HCl, 5 mM EGTA, 25 mM dithiothreitol, 2 % SDS, and 10 % glycerol with bromophenol blue as the tracking dye). Proteins were separated on 8 % SDS-polyacrylamide gels and transferred to nitrocellulose membranes. Blots were blocked overnight at 48 °C with 5 % non-fat dry milk dissolved in 20 mM Tris-HCl (pH 7.4), 150 mM NaCl, and 0.5 % Tween 20. p53 expression levels and caspase-3 cleavage were detected through incubation for 1 h with monoclonal anti-mouse against the p53 or monoclonal anti-mouse against (1:1000 in PBS), followed by incubation for 1 h with horseradish peroxidase-conjugated anti-mouse IgG (1:1500 in PBS). p53 expression and caspase-3 cleavage were visualized using a

SuperSignal West Pico Plus after autoradiography film exposure. Densitometric analysis was performed after normalization with anti-rabbit β -tubulin. View Article Online
DOI: 10.1039/C9OB00651F

Statistical analysis

Data were statistically analysed using one-way analysis of variance (one-way ANOVA) followed by post hoc Holm–Sidak test to estimate significant differences among groups. Data were reported as mean \pm SD of four experiments in duplicate, and differences between groups were considered to be significant at $*p < 0.05$.

Conflict of Interest

There are no conflicts to declare.

Acknowledgements

We gratefully acknowledge the Universities of Catania and Messina, Interuniversity Research Centre on Pericyclic Reactions and Synthesis of Hetero and Carbocycles Systems and the Interuniversity Consortium for Innovative Methodologies and Processes for Synthesis (CINMPIS) for partial financial support. The authors are very grateful to Professor Pierluigi Caramella for helpful discussion and suggestions.

REFERENCES

- (a) F. Bray, J. Ferlay, I. Soerjomataram, R. L. Siegel, L. A. Torre and A. Jemal, *CA- Cancer J. Clin.*, 2018, **68**, 394–424; (b) L. A. Torre, F. Islami, R. L. Siegel, E. M. Ward and A. Jemal, *Cancer Epidemiol. Biomarkers Prev.*, 2017, **26**, 444–457.
- (a) W. Yue, J. P. Wang, Y. Li, P. Fan, P.; G. Liu, N. Zhang, M. Conaway, H. Wang, K. S. Korach, W. Bocchinfuso and R. Santen, *Int. J. Cancer*, 2010, **127**, 1748–1756; (b) M. Chang, *Biomol. Ther.*, 2012, **20**, 256–267.
- D. W. Losordo and J. M. Isner, *Arterioscler Thromb Vasc Biol.*, 2001, **21**, 6–12.
- K. Subik, J. F. Lee, L. Baxter, T. Strzepek, D. Costello, P. Crowley, L. Xing, M. C. Hung, T. Bonfiglio, D. G. Hicks and P. Tang, *Breast Cancer*, 2010, **4**, 35–41.
- (a) L. Silwal-Pandit, H. K. Vollan, S. F. Chin, O. M. Rueda, S. McKinney, T. Osako, D. A. Quigley, V. N. Kristensen, S. Aparicio, A. L. Børresen-Dale, C. Caldas and A. Langerød, *Clin. Cancer Res.*, 2014; **20**:3569–80; (b) A. S. Coates, E. K. Millar, S. A. O’Toole, T. J. Molloy, G. Viale G, A. Goldhirsch, M. M. Regan, R. D. Gelber, Z. Sun, M. Castiglione-Gertsch, B. Gusterson, E. A. Musgrove and R. L. Sutherland RL, *Breast Cancer Res.*, 2012; **14**:R143.
- (a) C. M. Klinge, *Nucleic Acids Res.*, 2001, **29**, 2905–2919; (b) C. Y. Lin, A. Ström, V. B. Vega, S. L. Kong, A. L. Yeo, J. S. Thomsen, W. C. Chan, B. Doray, D. K. Bangarusamy, A. Ramasamy, L. A. Vergara, S. Tang, A. Chong, V. B. Bajic, L. D. Miller, J. A. Gustafsson and E. T. Liu, *Genome Biology*, 2004, **5**:R66.

- 7 (a) V. C. Jordan, I. Obiorah, P. Fan, H. R. Kim, E. Ariazi, H. Cunliffe and H. Brauch, *Breast*, 2011, **20**, 1–11; (b) D. Sharma, S. Kumar and B Narasimhan, *Chem. Cent. J.*, 2018, **12**:107, 1-32; (c) H. J. T. Coelingh Bennink, C. Verhoeven, A. E. Dutman and J. Thijssen, *Maturitas*, 2017, **95**, 11-23.
- 8 E. Giacomini, S. Rupiani, L. Guidotti, M. Recanatini and M. Roberti, *Curr. Med. Chem.*, 2016, **23**, 2439-2489.
- 9 K. M. Kasiotis and S- A. Haroutounian, *Curr. Org. Chem.*, 2012, **16**, 335-352.
- 10 S. Manna and M. H. Holz, *Sign Transduct Insights*, 2016, **5**, 1–7.
- 11 Y. C. Lim, L. Li, Z. Desta, Q. Zhao, J. M. Rae, D. A. Flockhart and T. C., *J. Pharmacol. Exp. Ther.*, 2006, **318**, 503-512.
- 12 B. M. Ford, L. N. Franks, A. Radominska-Pandya and P. L. Prathe, *PLOS ONE*, 2016, **11**, e0167240.
- 13 A. Detsi, M. Koufaki, and T. Calogeropoulou, *J. Org. Chem.*, 2002, **67**, 4608–4611.
- 14 C. K. Osborne, V. J. Wiebe, W. L. McGuire, D. R. Ciocca and M. W. De Gregorio, *J. Clin. Oncol.*, 1992, **10**, 304–310.
- 15 (a) R. Hu, L. Hilakivi-Clarke and R. Clarke, *Oncol. Lett.*, 2015, **9**, 1495–1501; (b) H. J. Pan, H. T. Chang and C. H. Lee, *J. Formos. Med. Association*, 2016, **115**, 411–417.
- 16 (a) Z. Qin, I. Kastrati, R. E. P. Chandrasena, H. Liu, P. Yao, P. A. Petukhov, J. L. Bolton and G. R. J. Thatcher, *J. Med. Chem.*, 2007, **50**, 2682–2692; (b) R. M. O'Regan, C. Gajdos, C. Dardes, A. De Los Reyes, W. Park, A. V. Rademaker and V. C., *JNCI-J. Natl. Cancer I.*, 2002, **94**, 274–283.
- 17 R. Abdelhamid, J. Luo, L. VandeVrede, I. Kundu, B. Michalsen, V. A. Litosh, I. T. Schiefer, T. Gherezghiher, P. Yao, Z. Qin and G. R. J. Thatcher, *ACS Chem. Neurosci.*, 2011, **2**, 256–268.
- 18 P. Kumar and Z. H. Song, *Biochem. Biophys. Res. Commun.*, 2014, **443**, 144-149.
- 19 S. Gauthier, J. Cloutier, Y. L. Dory, A. Favre, J. E. Mailhot, C. Ouellet, A. Schwerdtfeger, Y. Mérand, C. Martel, J. Simard and F. Labrie, *J. Enzyme Inhib. Med. Chem.*, 2005, **20**, 165–177.
- 20 D. G. Lloyd, R. B. Huges, D. M. Zisterer, D. C. Williams, C. Fattorusso, B. Catalanotti, G. Campiani and M. J. Meegan, *J. Med. Chem.*, 2004, **47**, 5612–5615.
- 21 A. Lukin, R. Karapetian, Y. Ivanenkov and M. Krasavin, *Lett. Drug Des. Discov.*, 2016, **13**, 198-204.
- 22 (a); (b) A. Piperno, A. Rescifina, A. Corsaro, M. A. Chiacchio, A. Procopio and R. Romeo, *Eur. J. Org. Chem.*, 2007, 1517- 1521; (c) A. Rescifina, M. A. Chiacchio, A. Corsaro, E. De Clercq, D. Iannazzo, A. Mastino, A. Piperno, G. Romeo, R. Romeo and V. Valveri, *J. Med. Chem.*, 2006, **49**, 709-715; (d) R. Romeo, S. V. Giofrè, A. Garozzo, B. Bisignano, A. Corsaro and M. A. Chiacchio, *Bioorganic Med. Chem.*, 2013, **21**, 5688–5693; (e) R Romeo, C. Carnovale, S. V. Giofrè, M. A.

Chiacchio, A. Garozzo, E. Amata, G. Romeo and U. Chiacchio, *Beilstein J. Org. Chem.*, 2015, **11**, 328-334. View Article Online
DOI: 10.1039/C5OB00651F

23 Y. Zhao and D. Truhlar, *Acc. Chem. Res.* 2008, **41**, 157-167

24 R. G. Parr, L. von Szentpály and S. Liu, *J. Am. Chem. Soc.*, 1999, **121**, 1922-1924.

25 L. R. Domingo, E. Chamorro and P. Pérez, *J. Org. Chem.*, 2008, **73**, 4615-4624.

26 (a) E. Chamorro, P. Perez, and L. R. Domingo, *Chem. Phys. Lett.*, 2013, **582**, 141-143. (b) P. Pérez, L. R. Domingo, M. José Aurell and R. Contreras, *Tetrahedron*, 2003, **59**, 3117-3125.

27 R. G. Parr and P. K. Chattaraj, *J. Am. Chem. Soc.*, 1991, **113**, 1854-1855.

28 A. Darù, D. Roca-López, T. Tejero and P. Merino, *J. Org. Chem.*, 2016, **81**, 673-680

29 (a) T. H. Jr. Dunning, *J. Chem. Phys.*, 1989, **90**, 1007-1023. (b) R. A. Kendall, T. H. Jr. Dunning and R. J. Harrison, *J. Chem. Phys.*, 1992, **96**, 6796-6806. (c) D. E. Woon, and T. H. Jr. Dunning, *J. Chem. Phys.*, 1993, **98**, 1358-1371.

30 (a) M. A. Chiacchio, L. Legnani, P. Caramella, T. Tejero and P. Merino *Eur. J. Org. Chem.* 2017, 1952-1960. (b) P. Merino, M. A. Chiacchio, L. Legnani, I. Delso and T. Tejero, *Org. Chem. Front.* 2017, **4**, 1541-1554. (c) M. A. Chiacchio, L. Legnani, P. Caramella, T. Tejero and P. Merino, *Tetrahedron*, 2018, **74**, 5627-5634.

31 M. J. Frisch, G. W. Trucks, H. B. Schlegel, G. E. Scuseria, M. A. Robb, J. R. Cheeseman, G. Scalmani, V. Barone, B. Mennucci, G. A. Petersson, H. Nakatsuji, M. Caricato, X. Li, H. P. Hratchian, A. F. Izmaylov, J. Bloino, G. Zheng, J. L. Sonnenberg, M. Hada, M. Ehara, K. Toyota, R. Fukuda, J. Hasegawa, M. Ishida, T. Nakajima, Y. Honda, O. Kitao, H. Nakai, T. Vreven, J. Montgomery, Jr., J. E. Peralta, F. Ogliaro, M. Bearpark, J. J. Heyd, E. Brothers, K. N. Kudin, V. N. Staroverov, R. Kobayashi, J. Normand, K. Raghavachari, A. Rendell, J. C. Burant, S. S. Iyengar, J. Tomasi, M. Cossi, N. Rega, J. M. Millam, M. Klene, J. E. Knox, J. B. Cross, V. Bakken, C. Adamo, J. Jaramillo, R. Gomperts, R. E. Stratmann, O. Yazyev, A. J. Austin, R. Cammi, C. Pomelli, J. W. Ochterski, R. L. Martin, K. Morokuma, V. G. Zakrzewski, G. A. Voth, P. Salvador, J. J. Dannenberg, S. Dapprich, A. D. Daniels, Ö. Farkas, J. B. Foresman, J. V. Ortiz, J. Cioslowski and D. J. Fox, Gaussian 09, Revision D.01, Gaussian, Inc., Wallingford CT, 2009.

32 (a) M. Muchtaridi, M. Yusuf, A. Diantini, S. B. Choi, B. O. Al-Najjar, J. V. Manurung, A. Subarnas, T. H. Achmad, S. R. Wardhani and H. A. Wahab, *Int. J. Mol. Sci.*, 2014, **15**, 7225-49; (b) M. Muchtaridi, H. N. Syahidah, A. Subarnas, M. Yusuf, S. D Bryant and T. Langer, *Pharmaceuticals*, 2017, **10**, 81 (12 pp).

33 A. Campisi, D. Caccamo, G. Li Volti, M. Currò, G. Parisi, R. Avola, A. Vanella and R. Ientile, *FEBS Lett.*, 2004, **578**, 80-84.

34 Romeo, S. V. Giofrè, C. Carnovale, A. Campisi, R. Parenti, L. Bandini and M. A. Chiacchio, *Bioorg Med Chem.*, 2013, **21**, 7929-7937.

35 A. Campisi, D. Caccamo, G. Raciti, G. Cannavò, V. Macaione, M. Currò, S. Macaione, A. Vanella and R. Ientile, *Brain Res.*, 2003, **978**, 24-30. View Article Online
DOI: 10.1039/C9OB00651F

36 R. Pellitteri, R. Bonfanti, M. Spatuzza, M. T. Cambria, M. Ferrara, G. Raciti and A. Campisi, *Mol. Neurobiol.*, 2017, **54**, 6785-6794.